



Improvement of hydrogen sorption properties of MgH_2 with various sizes and stoichiometric compositions of TiC

Jung Hoon Shin^{a,*}, Gil-Jae Lee^a, Young Whan Cho^b, Kyung Sub Lee^a

^a Division of Advanced Materials Science and Engineering, Hanyang University, Seoul 133-791, South Korea

^b Materials Science and Technology Research Division, Korea Institute of Science and Technology, Seoul 136-791, South Korea

ARTICLE INFO

Article history:

Available online 17 July 2009

Keywords:

Hydrogen storage
Magnesium hydride
Catalyst
TiC
Nanopowder

ABSTRACT

Nano TiC powders having various sizes (50 nm, 130 nm, 300 nm and 600 nm) were added to MgH_2 by high-energy ball milling to improve the hydrogenation properties of MgH_2 . The amount of hydrogen desorption/absorption of MgH_2 catalyzed with TiC was slightly decreased, but MgH_2 with 1 mol% TiC showed considerable catalytic effects on both the dehydrogenation and hydrogenation kinetics of MgH_2 .

MgH_2 with 50 nm TiC had the best absorption/desorption kinetics of MgH_2 and the highest cyclic performance, desorbing about 6.2 wt.% H_2 within about 20 min and absorbing more than 90% of hydrogen capacity within 5 min at 300 °C.

The size of TiC was the important factor in inducing the catalytic effect, but the change of TiC composition was not as important as the particle size. Because by changing of particle sizes of TiC led to significant progress of dehydrogenation, but there was neither improvement of hydrogenation properties nor reaction kinetics by variation of TiC composition.

X-ray diffraction analysis confirmed that nano-sized TiC remained stable with MgH_2 after five cyclic tests in accordance with the prediction of thermodynamic calculation.

© 2009 Elsevier B.V. All rights reserved.

1. Introduction

There have been many efforts to develop hydrogen storage materials that can meet effective capacity, reaction temperature, operating pressure and safety requirements at a reasonable cost [1]. Among the many hydrogen storage materials, magnesium and magnesium-based hydrides are the most promising. Magnesium hydride (MgH_2) has a theoretical hydrogen capacity of 7.6 wt.% and a volumetric density of 110 kg/m³. Its reversibility and cyclic performance are quite good compared with Group I and II binary and complex hydrides. Nevertheless, a high desorption temperature and slow sorption kinetics are the main problems to be overcome before MgH_2 can be seriously considered as a practical material for high capacity hydrogen storage systems [2–4]. Recently, with rapid developments in nanotechnology, there have been many efforts to reduce the dimensions of materials to nano-size in expectation of utilizing their unique properties that differ from those of bulk materials [5]. According to recent studies, substoichiometric MgH_2 has better diffusion properties than MgH_2 and it was considered that stoichiometric MgH_2 exist at grain

boundaries [6–8]. The sorption kinetics of MgH_2 has been dramatically improved by ball milling with some transition metals and oxides thereof [9–14]. In addition, the required milling time to achieve very fast sorption kinetics can be significantly reduced from a few days down to less than an hour or so by using Nb_2O_5 nanoparticles instead of ordinary micron-sized Nb_2O_5 powder [15]. Hanada et al. reported that the amount of hydrogen absorption reached up to about 4.5 wt.% at room temperature within 15 s for Mg catalyzed with meso-porous Nb_2O_5 [16]. It has been proposed that the actual catalytic effect has to be due either to metallic Nb or Mg–Nb composite oxides with probable oxygen deficiency formed during the first dehydrogenation/hydrogenation cycle [17,18]. Jung et al. [19] and Wang et al. [20] investigated the hydrogenation of MgH_2 catalyzed with various sized TiO_2 and found that hydrogen absorption kinetics and capacity were increased by forming the ultra fine nanocomposite of MgH_2 – TiO_2 . Borgschulte et al. [21] reported that surface composition and chemical state of MgH_2 that were changed by ball milling influenced the desorption kinetics of MgH_2 at high temperature. The hydrogen sorption kinetics of MgH_2 is found to be improved by increasing the number of catalytically active sites on the surface of the MgH_2 .

The aim of this study is to investigate the dehydrogenation/hydrogenation properties of MgH_2 catalyzed with a small amount

* Corresponding author. Tel.: +82 41 535 3445; fax: +82 2 2281 4914.
E-mail address: essinair@hotmail.com (J.H. Shin).

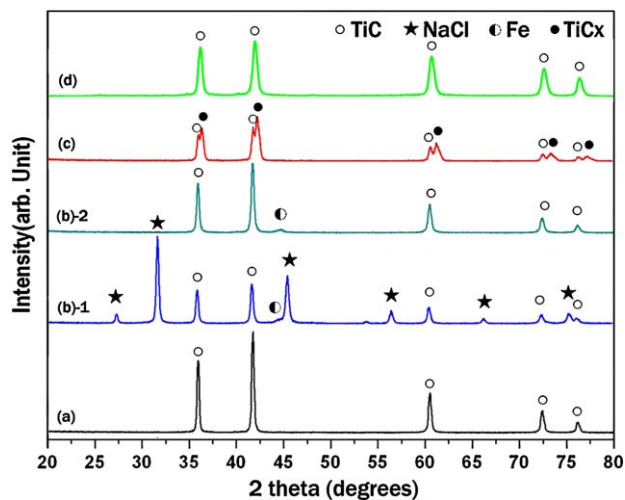


Fig. 1. XRD patterns of prepared sample (a) commercial 600 nm TiC, (b)-1 TiC with NaCl after milling for 4 h, (b)-2 TiC as filtered and dried from (b)-1, (c) commercial 130 nm TiC and (d) commercial 50 nm TiC.

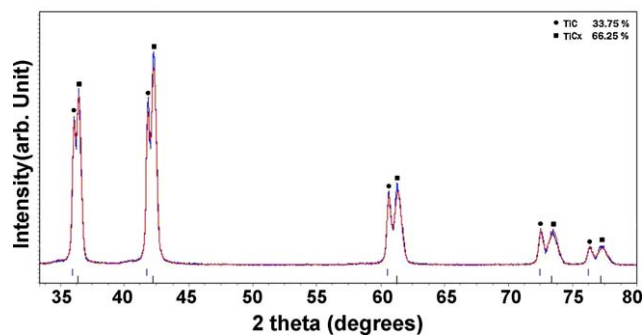


Fig. 2. Rietveld refinement of 130 nm TiC.

of TiC by high-energy ball milling in an attempt to improve the hydrogen storage capacity and kinetics of hydriding of Mg. The hydrogen properties of MgH_2 catalyzed TiC composites were investigated by X-ray diffraction (XRD), Thermogravimetry (TG) and a Sievert-type apparatus.

2. Experimental procedure

The starting material (MgH_2 , 99.8%) was purchased from Alfa-Aesar. Four types of TiC powder were adopted as catalysts; 600 nm

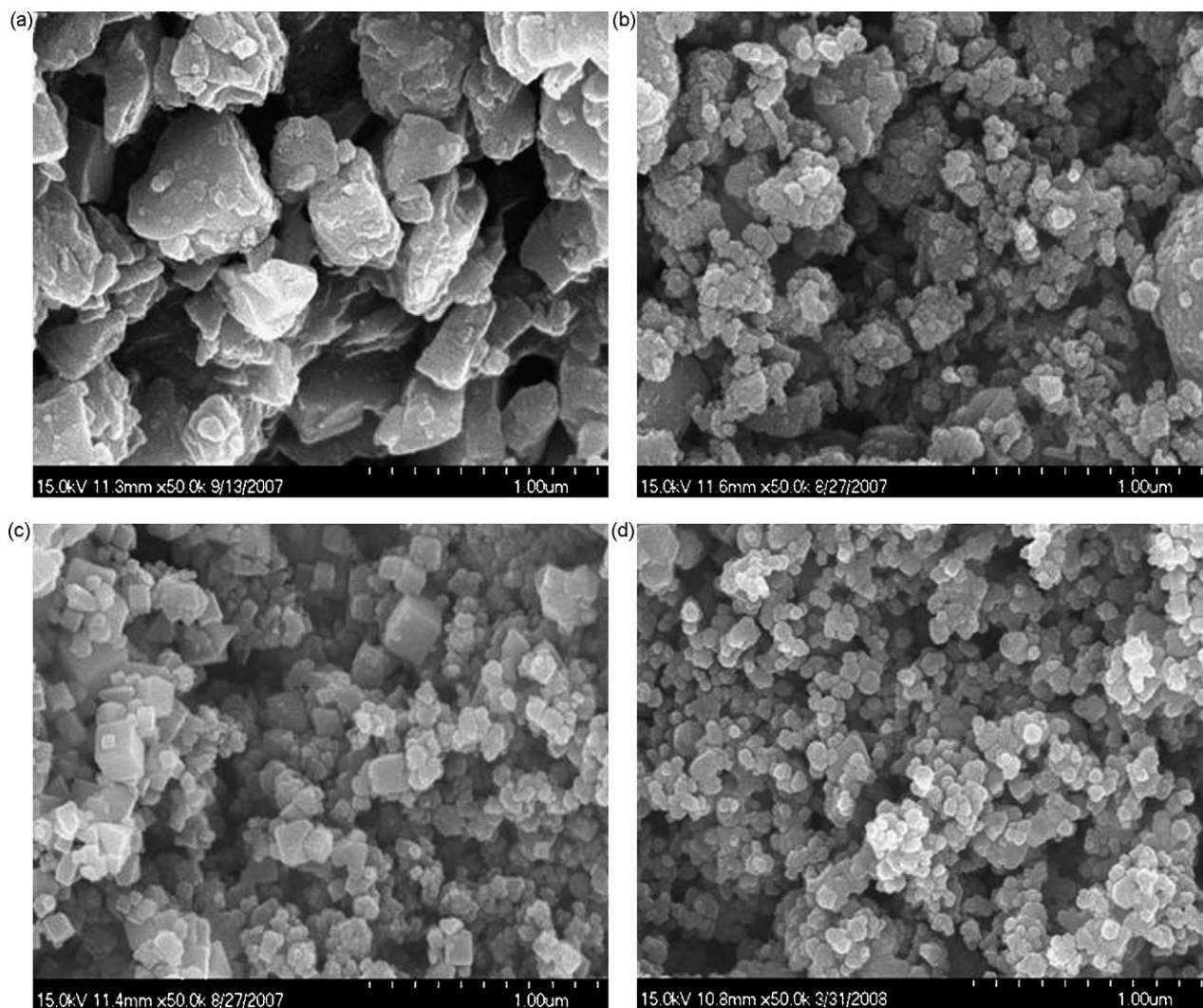


Fig. 3. SEM micrograph of the prepared TiC powder (a) commercial 600 nm TiC, (b) 300 nm TiC after additional milling, (c) commercial 130 nm TiC and (d) commercial 50 nm TiC.

(99%, Kojundo), 130 nm (98%, Sigma–Aldrich), 50 nm (99%, Alfa–Aesar) and 300 nm powder that was reduced from 600 nm TiC by ball milling using SPEX 8000 (ball to powder ratio 35:1). 50 vol.% NaCl (99.5, Junsei Chemical) was used as an inert process agent in milling, and it was removed by rinsing the milled powder in distilled water and filtering. The size of each TiC was observed by FE-SEM (Bruker).

Mixtures of MgH_2 and 1 mol% TiC were prepared. 1.5 g of each mixture was charged together with four 12.7 mm diameter (each 8.36 g) and fifteen 7.9 mm diameter (each 2.04 g) Cr-steel balls into a tool-steel vial under Ar atmosphere in a glove box and then milled in a Fritsch planetary (P7) for 4 h at 500 rpm. The milled powders were characterized by XRD using a Bruker D8 Advanced diffractometer with $\text{Cu K}\alpha$ radiation. In order to avoid exposure to air, the XRD samples were prepared in the glove box and a sample holder covered with an airtight plastic dome which had a negligible effect on diffraction patterns was used. The hydrogen desorption behavior of MgH_2 with catalyst was analyzed by TG using a NETSCH TG 209. The heating rate was $5^\circ\text{C}/\text{min}$ and the flow rate of 99.9999% Ar gas was 50 ml/min. Cyclic absorption and desorption of MgH_2 with and without catalyst were performed for 4 h at 300°C in a Sievert-type apparatus. The hydrogen absorption and desorption tests were, respectively, carried out under vacuum and about 10 bar hydrogen (99.9999%).

EPMA was used to investigate the distribution of TiC in the MgH_2 after milling. Elements of Ti, Mg and C were analyzed on the specimen that was pressed into pellet.

3. Thermodynamic analysis

In order to confirm if TiC remains thermodynamically stable with MgH_2 , thermodynamic equilibrium calculations of MgH_2 –1 mol% TiC from 0 to 500°C were carried out using the ThermoCalc. program [22]. Thermodynamic data of all the phase belonging to the Mg–H–Ti–C systems were taken from the SGTE substance database [23]. According to this calculation, it is expected that MgH_2 –1 mol% TiC composites decompose into Mg and H_2 gas at 280°C . The calculation results predict that TiC remain stable without any reaction in MgH_2 in the entire temperature range of 0– 500°C .

4. Results and discussion

Fig. 1 shows the XRD patterns of the prepared TiC powders. Fig. 2(a) is the commercial 600 nm TiC. NaCl that was added as PCA in ball milling 600 nm TiC to reduce it to 300 nm was confirmed to have been removed completely by rinsing and filtering in Fig. 2(b)–1 and (b)–2. A small amount of Fe found in the milled powders was probably due to contamination during milling. In the case of the 130 nm TiC, TiC_x as well as TiC was identified in Fig. 2(c). X value of TiC_x could be determined from the precise measurements of the lattice parameter of TiC_x since the lattice parameter of TiC_x varies with concentration of carbon in TiC_x .

The Rietveld refinements were carried out in Fig. 2 for the lattice parameter measurements which were estimated as 4.3241 \AA for TiC and 4.2799 \AA for TiC_x . X value of TiC_x was deduced to be about 0.9 from these measurements. The weight ratio of TiC to TiC_x was determined to be 33.75:66.25. It has been proposed that the vacancies are due to carbon deficiency in TiC_x and these vacancies could accelerate catalytic effects of TiC particles by dissociation of hydrogen molecules into hydrogen atoms and diffusion of hydrogen atoms through the interface between Mg and TiC. In order to prove this assumption, $\text{TiC}_{0.5}$ which had a higher concentration of vacancies was additionally prepared and hydrogenation properties were compared with TiC/ $\text{TiC}_{0.9}$. $\text{TiC}_{0.5}$ was synthesized from a mixture of TiCl_3 (99%, Sigma–Aldrich), CaC_2

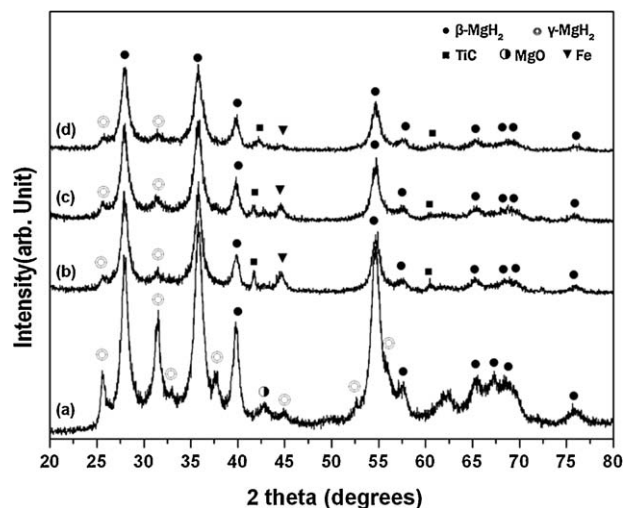


Fig. 4. XRD patterns of MgH_2 with and without catalyst after milling for 4 h (a) as-milled MgH_2 , (b) MgH_2 with 600 nm TiC, (c) MgH_2 with 300 nm TiC and (d) MgH_2 with 130 nm TiC.

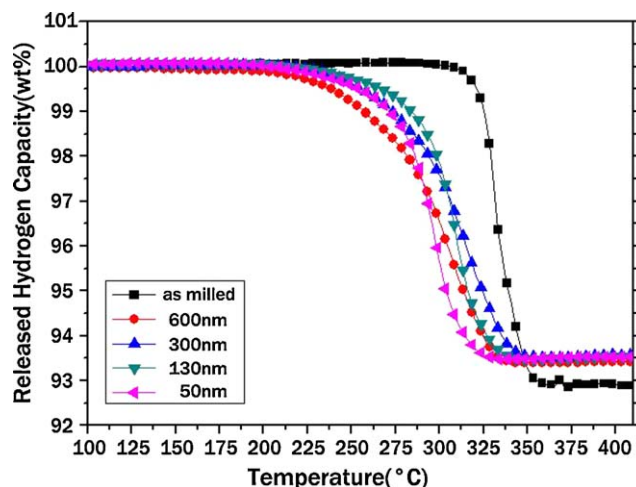


Fig. 5. TG curves of MgH_2 catalyzed with and without TiC.

(90%, Sigma–Aldrich) and Mg (98%, Alfa–Aesar) powders by high-energy ball milling for 4 h at 500 rpm using WC–Co balls with BPR 30:1. The milled powder was rinsed several times with distilled water, ethanol and acetone to remove salts (CaCl_2 and MgCl_2) and

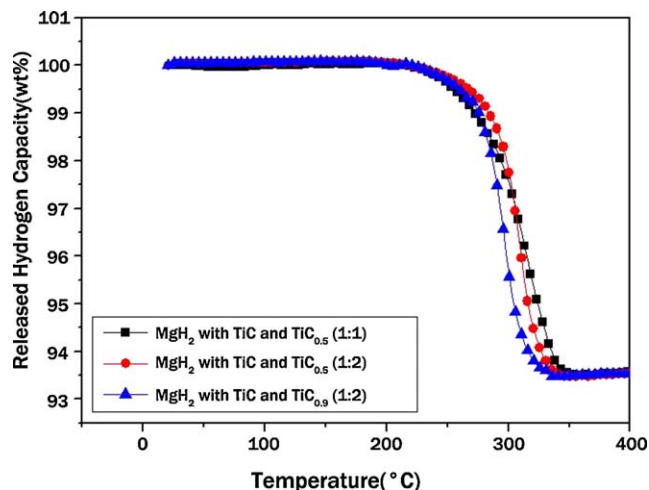


Fig. 6. TG curves of MgH_2 with TiC/ $\text{TiC}_{0.5}$ and TiC/ $\text{TiC}_{0.9}$.

filtered through a cellulose acetate membrane. $\text{TiC}_{0.5}$ was mixed with TiC in the ratios of 1:1 and 2:1, and ball milled with MgH_2 using the same method as other samples.

Fig. 3 shows SEM micrographs of various sized TiC powders. All the particles exhibited an irregular shape and appeared slightly agglomerated. The primary particle sizes of commercial TiC powders were about, Fig. 4 (a) 600 nm, (c) 130 nm and (d) 50 nm, respectively. The commercial 600 nm TiC was reduced to

about 300 nm after only 4 h of additional milling with NaCl (Fig. 5(b)).

XRD patterns of MgH_2 with TiC after ball milling for 4 h are presented in Fig. 4. TiC remained stable in MgH_2 indicating no reaction with MgH_2 in accordance with the thermodynamic calculation. Thus, it is expected that TiC would not incur any significant loss of the hydrogen storage capacity of MgH_2 . $\beta\text{-MgH}_2$ is the equilibrium phase at room temperature; however both

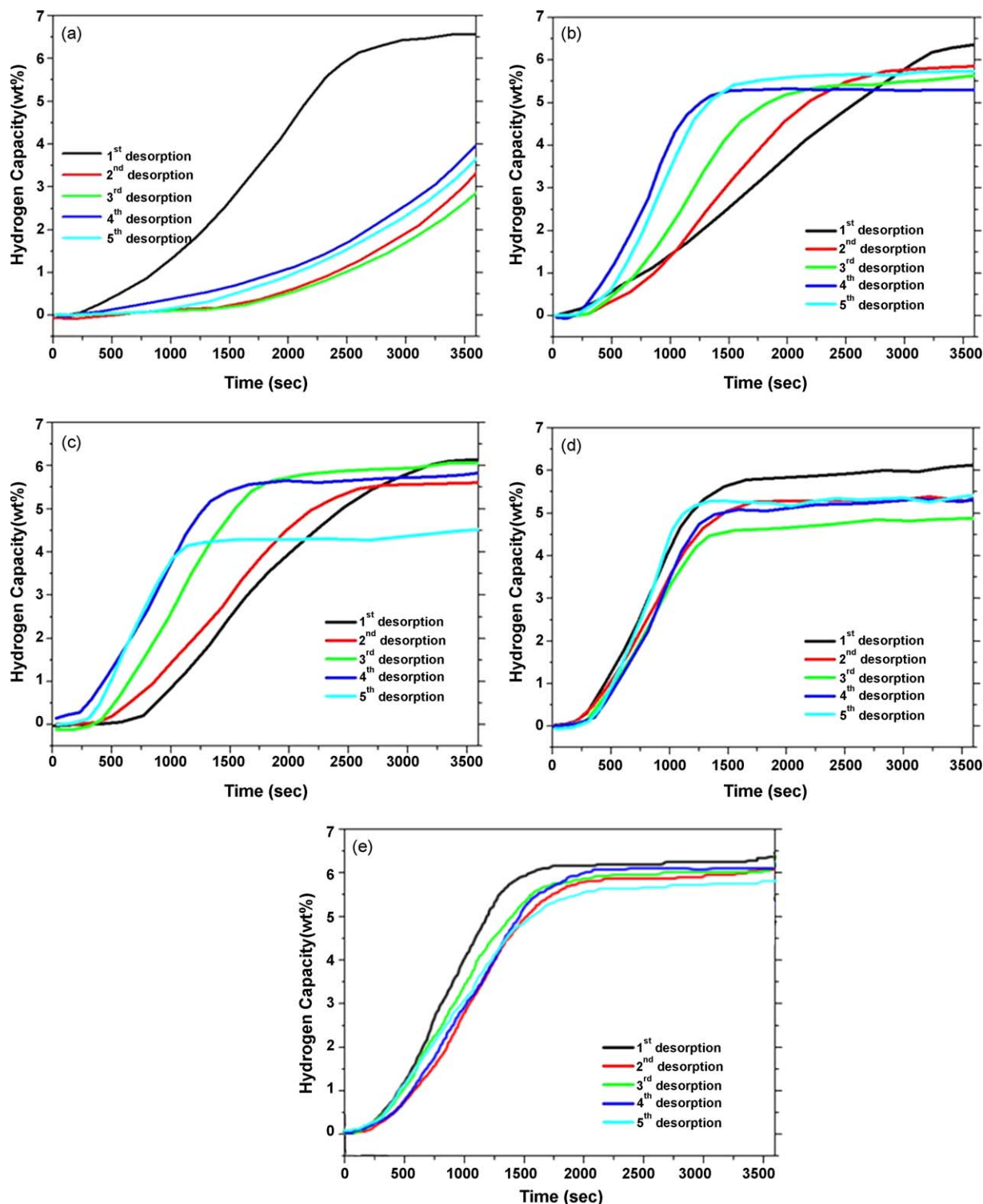


Fig. 7. Hydrogen desorption curves for five cycles of (a) as-milled MgH_2 , (b) MgH_2 with 600 nm TiC, (c) MgH_2 with 300 nm TiC, (d) MgH_2 with 130 nm TiC and (e) MgH_2 with 50 nm TiC at 300 °C.

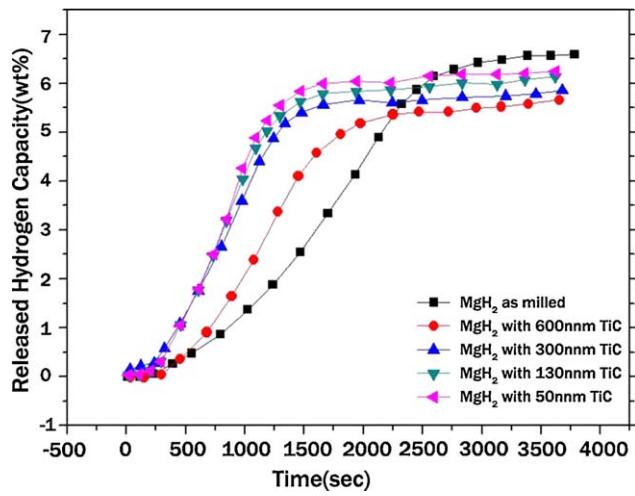


Fig. 8. Hydrogen desorption curves of MgH_2 catalyzed with and without TiC.

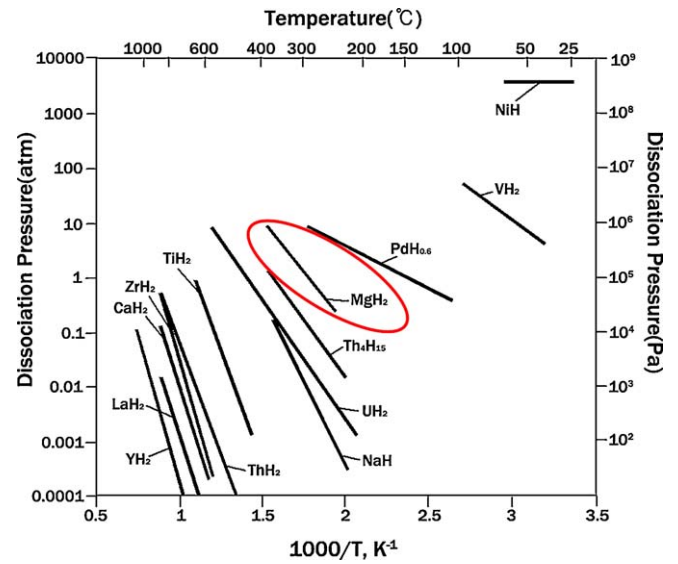


Fig. 9. Van't Hoff plot for elemental hydrides (desorption).

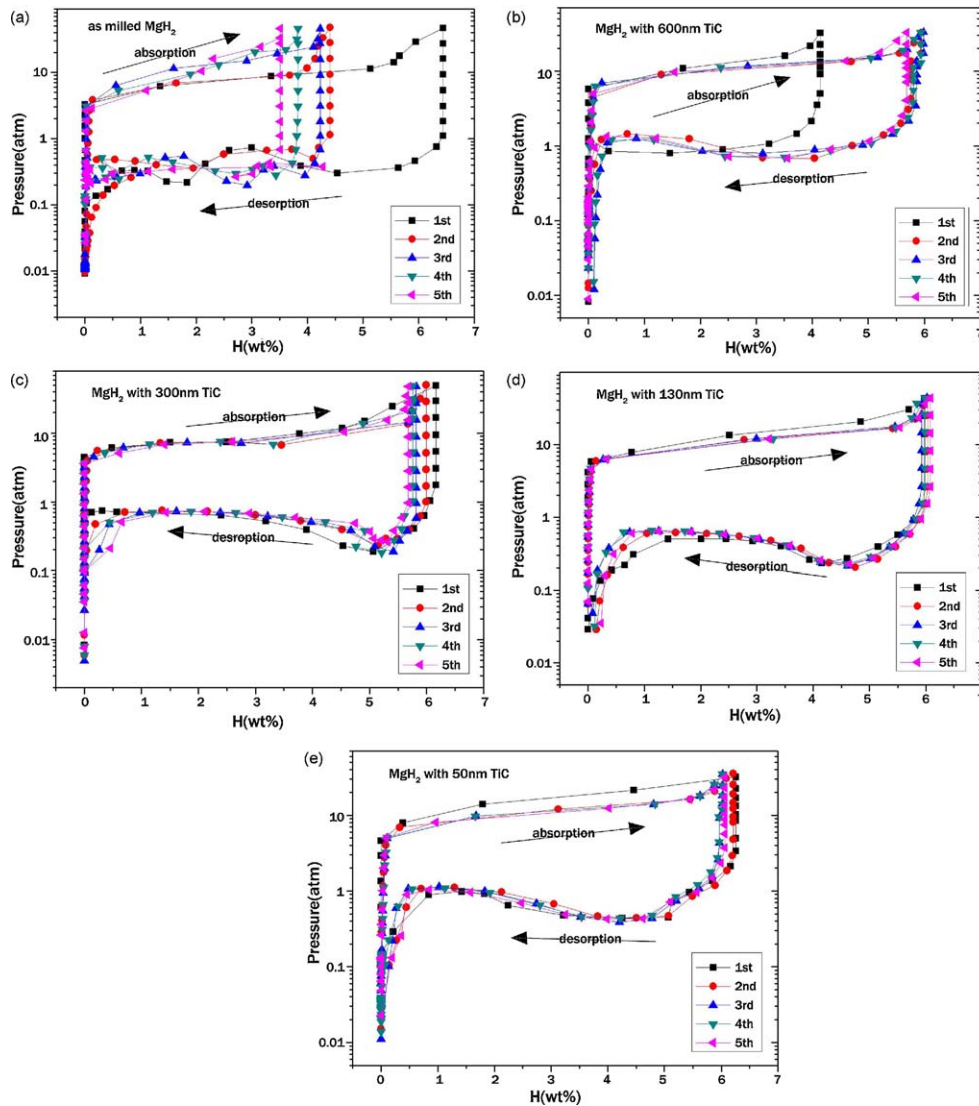


Fig. 10. Cycle curves of absorption and desorption of (a) as-milled MgH_2 , (b) MgH_2 with 600 nm TiC, (c) MgH_2 with 300 nm TiC, (d) MgH_2 with 130 nm TiC and (e) MgH_2 with 50 nm TiC.

tetragonal (β) and orthorhombic (γ) MgH_2 were observed in all the samples after milling, together with a small amount of MgO which was also detected in the as-received MgH_2 . Also, a small amount of Fe as an impurity was present.

Fig. 5 shows that the as-milled MgH_2 started to desorb H_2 at 307 °C and finished decomposition at 358 °C. The starting temperature was lower than that of annealed un-milled MgH_2 owing to the strain energy from the ball milling; however, the finishing temperature was almost the same. With the TiC, the decomposition starting temperature decreased to 199 °C from 307 °C as the size of the TiC reduced, but the finishing temperature at which the hydrogen was fully released decreased to 326 °C from 358 °C. The catalytic effect of TiC was evident in reducing the decomposition temperature of MgH_2 , being more pronounced in the decomposition starting temperature. The area under the TG curve can be used to estimate the total thermal energy required for the reaction. From the comparison of the areas of the decomposition curve, it can be observed that less thermal energy was required for the decomposition of MgH_2 with the TiC.

Fig. 6 shows the result of effect vacancy concentration in the TiC on hydrogenation of MgH_2 measured by TG. There was no significant change of hydrogen capacity or decomposition temperature between $\text{TiC}/\text{TiC}_{0.5}$ (1:1) and $\text{TiC}/\text{TiC}_{0.5}$ (1:2), both had the size of about 250–300 nm. $\text{TiC}/\text{TiC}_{0.9}$ which had a lower vacancy concentration than $\text{TiC}/\text{TiC}_{0.5}$, but a smaller size (130 nm) showed a slight decrease of decomposition temperature and thermal energy to desorb hydrogen. It can therefore be inferred from these results that the non-stoichiometry (vacancy concentration) of TiC was not the determining factor as the particle size of TiC in incurring the catalytic effect.

Fig. 7 shows the cyclic performance of MgH_2 with TiC at 300 °C measured by a Sievert-type apparatus for initial five cycles. The capacity of H_2 desorption of as-milled MgH_2 deteriorated quickly to 4 wt.% from 6.6 wt.% in 2–5 cycles and the kinetics were also reduced from 2.8344×10^{-3} wt.%/s to 1.1765×10^{-3} wt.%/s. Meanwhile, MgH_2 with TiC exhibited almost the same amount of hydrogen absorption and the same level of kinetics, about 6×10^{-3} wt.%/s with cycles. Although measured in the limited cycles, the beneficial effects of TiC catalysts in MgH_2 were clearly demonstrated in the cyclic performance.

Fig. 8 compares the maximum hydrogen capacity and the time to reach the maximum measured at 300 °C. As-milled MgH_2 desorbed 6.6 wt.% of hydrogen in about 3000 s but MgH_2 with 50 nm was 6.4 wt.% in about 1700 s. It was found that the smaller the TiC size the higher the hydrogen desorption kinetics resulted. Desorption time decreased as the size of TiC was reduced. It is obvious from this result that the smaller the particle size, the faster the kinetics.

The equilibrium conditions of the PCT experiments were set up from Fig. 9 [24]. MgH_2 with no catalyst absorbs and desorbs the hydrogen almost 300 °C at 1 atm. So that hydrogen absorption and desorption be processes properly, PCT measurements were operated at 300 °C.

Fig. 10 shows the PCT curves of (a) as-milled MgH_2 , (b) MgH_2 with 600 nm TiC, (c) MgH_2 with 300 nm TiC, (d) MgH_2 with 130 nm TiC and (e) MgH_2 with 50 nm TiC measured at 300 °C. Before PCT measurements, all the samples were operated decomposition and activation process for 12 h at 400 °C. Then five repetitions of absorption and desorption (cycles) were performed for about 3 h each cycle. There was no significant change in plateau pressures with cycles in MgH_2 with or without TiC. The plateau pressure of absorption was about 8–9 atm and desorption was about 0.8–1.0 atm in all the samples. Fast degradation of MgH_2 without TiC with cycles was again displayed in this figure.

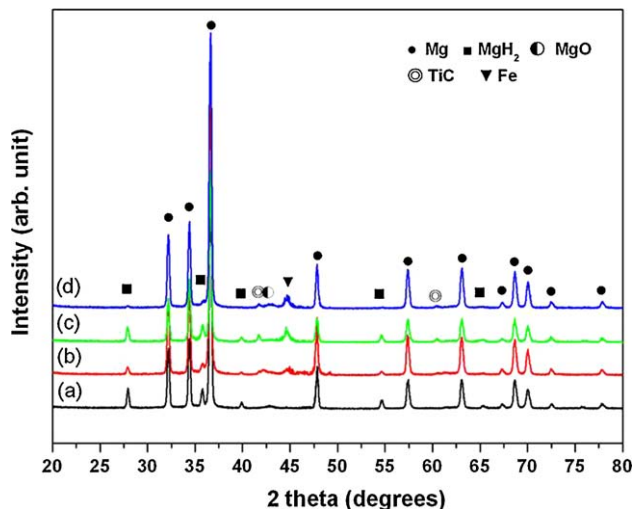


Fig. 11. XRD patterns of MgH_2 with and without catalyst after five cycles.

XRD patterns of MgH_2 with and without TiC after cyclic tests are shown in Fig. 11. As predicted from the thermodynamic calculation, TiC did not react with MgH_2 during the cycle. Apart from MgH_2 with 130 nm TiC, all the samples showed a small amount of undecomposed MgH_2 due to the incomplete decomposition of MgH_2 . The complete decomposition of MgH_2 with 50 nm TiC under identical testing conditions further shows that the catalytic effect improves as the size of the catalyst decreases.

5. Conclusion

Hydrogenation properties of MgH_2 catalyzed with various sized TiC by high-energy ball milling were investigated. The hydrogen absorption/desorption kinetics were increased and the cyclic performance improved as the size of the catalysts decreased. Hydrogen desorption starting temperature and total thermal energy required for the complete desorption of MgH_2 were also reduced with the TiC catalyst. High concentration vacancies in TiC showed little catalytic effect on the hydrogenation properties of Mg.

References

- [1] L. Schlögl, A. Züttel, *Nature* 414 (2002) 353.
- [2] J. Huot, M.L. Tremblay, R. Schulz, *J. Alloys Compd.* 356/357 (2003) 603.
- [3] J.L. Bobet, S. Desmoulin-Krawiec, E. Grigorova, R. Cansell, B. Chevalier, *J. Alloys Compd.* 351 (2003) 217.
- [4] A. Zaluski, L. Zaluski, *J. Alloys Compd.* 404–406 (2005) 709.
- [5] M.C. Roco, *J. Nanoparticle Res.* 1 (1–6) (1999).
- [6] H. Gijss Schimmel, J. Huot, L.C. Cahoon, F.D. Tichelaar, F.M. Mulder, *J. Am. Chem. Soc.* 127 (2005) 14348.
- [7] C.W. Ostendorf, M. Johansson, I. Chorkendorff, *Surf. Sci.* 601 (2007) 1862.
- [8] A. Borgshulte, U. Boesenberg, G. Barkhordarian, M. Dornheim, R. Bormann, *Catal. Today* 120 (2007) 262.
- [9] A. Zaluska, L. Zaluski, J.O. Strom-Olson, *J. Alloys Compd.* 289 (1999) 197.
- [10] G. Liang, J. Huot, S. Boily, A. van Neste, R. Schulz, *J. Alloys Compd.* 291 (1999) 295.
- [11] W. Oelerich, T. Klassen, R. Bormann, *J. Alloys Compd.* 315 (2001) 237.
- [12] G. Barkhordarian, T. Klassen, R. Bormann, *Scr. Mater.* 49 (2003) 213.
- [13] O. Friedrichs, T. Klassen, J.C. Sanchez-Lopez, R. Bormann, A. Fernandez, *Scr. Mater.* 54 (2006) 1293.
- [14] O. Friedrichs, F. Aguey-Zinsou, J.R. Fernandez, J.C. Sanchez-Lopez, A. Justo, T. Klassen, R. Bormann, A. Fernandez, *Acta Mater.* 54 (2006) 105.
- [15] E. Ivanov, I. Konstantchuk, B. Bokhonov, V. Boldyre, *J. Alloys Compd.* 359 (2003) 320.
- [16] J.F.R. de Castro, A.R. Yavari, A. LeMoulec, T.T. Ishikawa, W.J. Botta, *J. Alloys Compd.* 389 (2005) 270.
- [17] A.R. Yavari, A. LeMoulec, J.F.R. de Castro, S. Deledda, O. Friedrichs, W.J. Botta, G. Vanghan, T. Klassen, A. Fernandez, A. Kvick, *Scr. Mater.* 52 (2005) 719.
- [18] S. Deledda, A. Borissova, C. Poinsignon, W.J. Botta, M. Dornheim, T. Klassen, *J. Alloys Compd.* 404–406 (2005) 409.

- [19] K.S. Jung, D.H. Kim, E.Y. Lee, K.S. Lee, Catal. Today 120 (2007) 270.
- [20] P. Wang, A.M. Wang, H.F. Zhang, B.Z. Ding, Z.Q. Hu, J. Alloys Compd. 313 (2000) 218.
- [21] A. Borgschulte, M. Biemann, A. Züttel, G. Barkhodarian, M. Dornheim, R. Borrmann, Appl. Surf. Sci. 254 (2008) 2377.
- [22] <http://www.thermocalc.se>.
- [23] B.M. Lee, J.W. Jang, J.H. Shim, Y.W. Cho, B.J. Lee, J. Alloys Compd. 424 (2006) 370.
- [24] R. Grisson, Hydrogen in Intermetallic Compounds, I and II, Springer-Verlag, 1988., p. 219.